

We have now completed our survey of the physical processes that govern the behaviour of stars, and we are ready to build a theory for stars' structure and evolution. This class will focus on the main sequence, and the next two will focus on evolution past the main sequence. In modern day applications, quantitative models of stars are invariably obtained by solving the stellar structure equations numerically, and we will look at numerical results at the end of the class. However, to get physical insight into why the numerical results look like they do, we will first attempt to proceed as far as we can analytically.

### I. The conditions in stellar centres

We will begin our study by considering the properties of stars' centres, which we can characterise in terms of a density  $\rho_c$ , a temperature  $T_c$ , and a composition. Imagine we consider a series of stars of different masses, we find their central temperatures and densities, and we plot them in a plane of  $(\log T_c, \log \rho_c)$ . Where will the stars lie in the  $(\log T_c, \log \rho_c)$ -plane, and why?

Our central hypothesis is that main sequence stars represent systems that are in both hydrostatic and energy equilibrium, meaning that their internal pressure hold them up, and their internal rates of nuclear energy generation match their rates of radiation into space. Let us therefore see what these two conditions imply about the properties of stars' centres.

#### A. Hydrostatic balance

First let us consider where in this plane hydrostatic balance is possible. Since we care about pressures for hydrostatic balance, it is helpful to remind ourselves of the different sources of pressure, and where in terms of density and temperature each one dominates. Using the expressions for various types of pressure that we have derived previously, we can populate the  $(\log T_c, \log \rho_c)$  plane to demarcate where each type of pressure dominates, as shown in [Figure 1](#).

To figure this out where stars fall in this plane, we can take advantage of the powerful and general relationship between mass, pressure, and central density for polytropes. Recall that for a polytrope characterised by a pressure-density relationship  $P = K_P \rho^{(n+1)/n}$ , we showed that the mass and central density are related by:

$$M = -4\pi\alpha^3\rho_c\xi_1^2\left(\frac{d\Theta}{d\xi}\right)_{\xi_1} \quad (1)$$

$$\alpha = \left[\frac{(n+1)K_P}{4\pi G\rho_c^{(n-1)/n}}\right]^{1/2} \quad (2)$$

where  $\xi_1$  and  $(d\Theta/d\xi)_{\xi_1}$  are numerical values of order unity that depend only on the index  $n$ .

To figure out the central temperature, we need to know the central pressure, so let us combine the above two expressions and see if we can get an expression for the pressure in terms of  $M$  and  $\rho_c$  by eliminating  $K_P$ . This is fairly straightforward:

$$M = -4\pi\left[\frac{(n+1)K_P}{4\pi G\rho_c^{(n-1)/n}}\right]^{3/2}\rho_c\xi_1^2\left(\frac{d\Theta}{d\xi}\right)_{\xi_1} \quad (3)$$

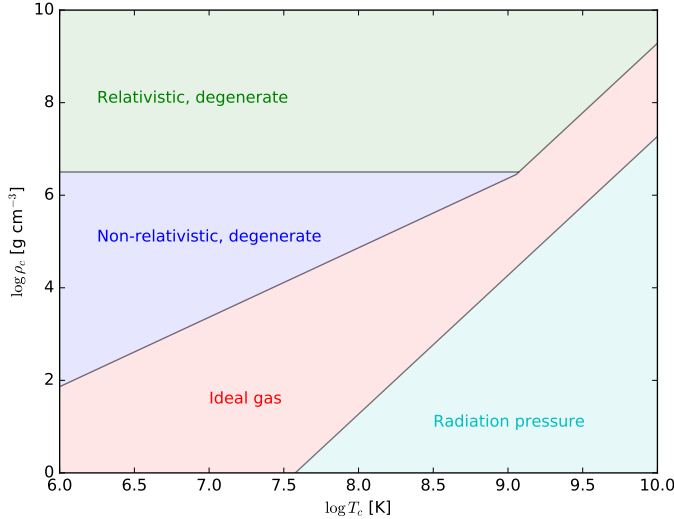


Figure 1: Sources of pressure in the temperature-density plane. The shaded regions indicate roughly where different types of pressure become dominant.

$$M = -4\pi \left[ \frac{(n+1)P_c \rho_c^{-(n+1)/n}}{4\pi G \rho_c^{(n-1)/n}} \right]^{3/2} \rho_c \xi_1^2 \left( \frac{d\Theta}{d\xi} \right)_{\xi_1} \quad (4)$$

$$= - \left[ \frac{(n+1)^3}{4\pi G^3} \right]^{1/2} \frac{P_c^{3/2}}{\rho_c^2} \xi_1^2 \left( \frac{d\Theta}{d\xi} \right)_{\xi_1} \quad (5)$$

Re-arranging, we see that

$$P_c = (4\pi)^{1/3} B_n G M^{3/2} \rho_c^{4/3} \quad (6)$$

where  $B_n$  is a constant of order unity that just depends on  $n$ .

Real stars aren't exactly polytropes except in certain special cases, but we have shown that their structures are generally bounded between  $n = 1.5$  and  $n = 3$  polytropes, depending on the strength of convection and the amount of pressure provided by radiation. For an  $n = 1.5$  polytrope,  $B_n = 0.206$ , and for one with  $n = 3$ ,  $B_n = 0.157$ . That these values are so close suggests that this equation should apply in general, with only a slight dependence of the coefficient on the internal structure of the star. For this reason, we can simply adopt an approximate value  $B_n \simeq 0.2$ , and expect that it won't be too far off for most stars.

In order to translate this relationship between  $P_c$  and  $\rho_c$  into our  $(\log T, \log \rho)$  plane, we need to compute the central temperature  $T_c$  from  $\rho_c$  and  $P_c$ . This in turn requires that we use the equation of state. We've discussed the equation of state in a few limiting cases, but, as we will see for a moment, for most main sequence stars we really only need to worry about two cases: ideal gas and non-relativistic degenerate gas. That is because stars that get too far into one of the other two regimes, either relativistic degenerate gas or radiation pressure, become unstable, as we will see.

For an ideal gas, we have

$$P_c = \frac{\mathcal{R}}{\mu} \rho_c T_c, \quad (7)$$

so combining this with the central pressure-density relation, we have

$$\frac{\mathcal{R}}{\mu} \rho_c T_c = (4\pi)^{1/3} B_n G M^{2/3} \rho_c^{4/3} \quad (8)$$

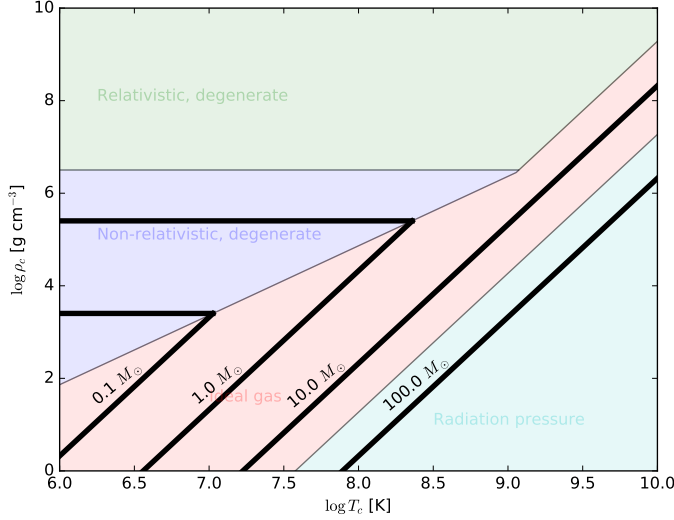


Figure 2: Thick lines show loci where stars of the indicated mass can be in hydrostatic equilibrium, plotted on top of shaded regions indicating sources of pressure, as in Figure 1.

$$\rho_c = \frac{1}{4\pi B_n^3} \left( \frac{\mathcal{R}}{\mu} \right)^3 \frac{1}{G^3 M^2} T_c^3 \quad (9)$$

$$\log \rho_c = 3 \log T_c - 2 \log M - 3 \log G - \log(4\pi B_n^3) + 3 \log \frac{\mathcal{R}}{\mu}. \quad (10)$$

Thus in the case of an ideal gas, the relationship between central density and temperature is simply a line of slope 3 in our  $(\log \rho_c, \log T_c)$  plane. The  $y$  intercept of the line depends on the star's mass  $M$ , so that stars of different masses simply lie along a set of parallel lines.

If the gas is instead degenerate, we showed that the equation of state is

$$P_c = K'_1 \left( \frac{\rho_c}{\mu_e} \right)^{5/3}. \quad (11)$$

Repeating the same trick of combining this with the polytropic pressure-density relation, we have

$$K'_1 \left( \frac{\rho_c}{\mu_e} \right)^{5/3} = (4\pi)^{1/3} B_n G M^{2/3} \rho_c^{4/3} \quad (12)$$

$$\rho_c = 4\pi B_n^3 G^3 M^2 K_1'^{-3} \mu_e^5 \quad (13)$$

$$\log \rho_c = \log(4\pi B_n^3) - 3 \log K'_1 + 5 \log \mu_e + 3 \log G + 2 \log M \quad (14)$$

This is just a horizontal line in the  $(\log \rho_c, \log T_c)$  plane, at a value that depends on the star's mass  $M$ . The crossover between degenerate and non-degenerate occurs where this horizontal line crosses the line of slope 3 we obtained for the non-degenerate case.

Figure 2 shows the lines of hydrostatic equilibrium in the  $(\log T_c, \log \rho_c)$  plane. We see that 0.1 and 1.0  $M_\odot$  stars can be either ideal gases or degenerate in their centres, while 10  $M_\odot$  are essentially always ideal gasses. This plot shows that our calculation for 100  $M_\odot$  stars isn't quite right, since these are in the region that should be dominated by radiation pressure, but we will ignore this for now, because the correction is not that large, and does not become significant except for the most massive stars.

## B. Energy equilibrium

Now that we know what where stars can be in hydrostatic balance on this plot, the next thing to add is where they can be in energy balance, meaning where their rate of nuclear energy generation matches their rate of radiative loss into space. As with our calculation of hydrostatic equilibrium, we will proceed by very rough approximation.

For an ideal gas the energy per unit mass is

$$u_{\text{gas}} = \frac{3}{2} \frac{P_{\text{gas}}}{\rho} = \frac{3}{2} \frac{\mathcal{R}}{\mu} T. \quad (15)$$

The time it takes the gas to lose energy via radiation is the Kelvin-Helmholtz timescale, so the time rate of change of the energy per unit mass due to radiative loss is

$$\left( \frac{du_{\text{gas}}}{dt} \right)_{\text{rad}} \sim \frac{\mathcal{R}}{\mu} \frac{T}{t_{\text{KH}}}. \quad (16)$$

The KH timescale is a fairly strong function of stellar mass as it turns out, but so is the central temperature, and so it turns out that the ratio  $T/t_{\text{KH}}$  only varies by a factor of  $\sim 10$  across the main sequence. That is good enough for this very schematic calculation, so we'll plug in Solar central values of  $T \sim 10^7$  K and  $t_{\text{KH}} \sim 10$  Myr, giving  $(du_{\text{gas}}/dt)_{\text{rad}} \sim 10 \text{ erg g}^{-1} \text{ s}^{-1}$  as the rate of radiative loss.

In energy equilibrium this loss must be balanced by the rate of nuclear energy generation per unit mass. Recall that we previously computed these rates from the  $pp$  chain and the CNO cycle:

$$q_{pp} \simeq 2.4 \times 10^6 X^2 \left( \frac{\rho}{1 \text{ g cm}^{-3}} \right) \left( \frac{T}{10^6 \text{ K}} \right)^{-2/3} \exp \left[ -\frac{33.8}{(T/10^6 \text{ K})^{1/3}} \right] \quad (17)$$

$$q_{\text{CNO}} \simeq 8.7 \times 10^{27} X X_{\text{CNO}} \left( \frac{\rho}{1 \text{ g cm}^{-3}} \right) \left( \frac{T}{10^6 \text{ K}} \right)^{-2/3} \exp \left[ -\frac{152}{(T/10^6 \text{ K})^{1/3}} \right] \quad (18)$$

If we equate these rates with  $(du_{\text{gas}}/dt)_{\text{rad}}$  and take the logarithm to figure out what this looks like in the  $(\log T_c, \log \rho_c)$  plane, the result is

$$\log \rho_{pp} = 14.7 T_6^{-1/3} + \frac{2}{3} \log T_6 - 6.4 - 2 \log X + \log \left( \frac{du_{\text{gas}}}{dt} \right)_{\text{rad}} \quad (19)$$

$$\log \rho_{\text{CNO}} = 66.0 T_6^{-1/3} + \frac{2}{3} \log T_6 - 27.9 - \log X - \log X_{\text{CNO}} + \log \left( \frac{du_{\text{gas}}}{dt} \right)_{\text{rad}} \quad (20)$$

where we have used the abbreviation  $T_n = T/(10^n \text{ K})$ . These are clearly not straight lines in the  $(\log T_c, \log \rho_c)$  plane. There is a linear part, which comes from the  $(2/3) \log T$  terms, but there is a far more important exponential part, coming from the  $T^{-1/3}$  terms, which look like exponentials in the  $(\log T_c, \log \rho_c)$  plane. If we adopt  $X = 0.71$  and  $X_{\text{CNO}} = 0.01$  as for the Sun, we can add these curves to our plot, as shown in [Figure 3](#).

### C. Implications for the main sequence

[Figure 3](#) provides great insight into how stars must evolve, and into the origin of the main sequence. First note that, as long as a star's mass remains fixed, it is constrained to spend its entire life somewhere on the line associated with its mass – it simply moves from one point on the line to another.

Now consider how a star must evolve when it first forms. Stars form out of gas clouds that are much less dense and much colder than the centre of a star.

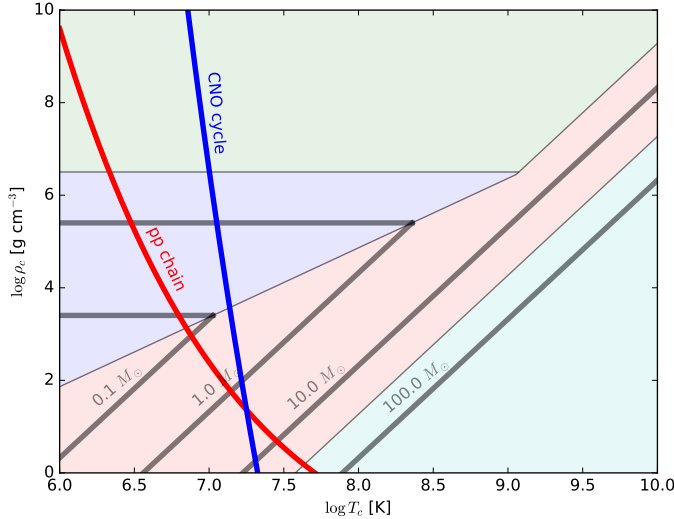


Figure 3: Red and blue lines show the loci where nuclear burning through the  $pp$  chain (red) and CNO cycle (blue) are sufficient to produce energy equilibrium in a star radiating away energy at a rate per unit mass  $du_{\text{gas}}/dt \sim 10 \text{ erg g s}^{-1}$ , roughly the value for the Sun. Thick gray lines show loci where stars of the indicated mass can be in hydrostatic equilibrium, while shaded regions indicate sources of pressure, as in Figure 2.

Thus all stars begin their lives at the bottom left corner of the diagram. Since they are at a temperature too low to balance their radiative losses (since they are to the left of the  $pp$  chain and CNO cycle lines where balance occurs), their radiation must be powered by gravitational contraction instead, and their densities rise. Thus they move up and to the right along the ideal gas track.

They continue to move in this way until one of three things happens. Stars much below  $0.1 M_{\odot}$  will hit the degenerate region before hitting any of the nuclear burning lines. At this point its central density will cease contracting; it cannot rise any more. Since it is still losing energy to space, it will continue to evolve, but now it will move back toward lower temperature, proceeding left on its track. Objects in this category are called brown dwarfs; they never get hot enough to burn hydrogen.

Slightly more massive stars will hit the  $pp$  chain line before this happens, while stars larger than a few  $M_{\odot}$  will hit the CNO cycle line first. Once either of these two things happens, the star will stop evolving, because it will not be in energy balance, with nuclear burning balancing the loss of energy to space. Eventually the equilibrium will fail because hydrogen will be exhausted and the rates of nuclear energy generation will decline, but this requires a nuclear burning timescale to happen, which for low mass stars like the Sun is very long,  $\sim 10 \text{ Gyr}$ .

Thus stars stall along a locus in the  $(\log T_c, \log \rho_c)$  plane defined by the intersection of their mass tracks with the nuclear burning lines. This is the locus that will define the main sequence.

We can already see just from the plot a few interesting things. First, more massive stars will tend to have higher central temperatures but lower central densities than less massive stars. Second, they will be closer to the region where radiation pressure dominates, and thus radiation pressure will become increasingly important for more massive stars.

## II. Scaling relations on the main sequence

Having understood the origin of the main sequence in terms of the properties of stellar cores, we next seek to develop a more quantitative understanding of main sequence stars' properties. We are particularly interested in understanding how luminosity and effective

temperature scale with mass, since that is what gives us the relationship between the observational main sequence (defined in terms of an observed luminosity and effective temperature) and the physical properties of a star, particularly its mass.

#### A. Non-dimensional structure equations

To proceed analytically, we again need to make approximations. To this end, we will neglect convection, radiation pressure, and degeneracy pressure, use a constant opacity, and use a powerlaw approximation for the rate of nuclear burning. The goal is to show that we can roughly reproduce what is observed, not get every detail right. With these assumptions, the complete set of stellar structure equations is

$$\frac{dP}{dm} = -\frac{Gm}{4\pi r^4} \quad (21)$$

$$\frac{dr}{dm} = \frac{1}{4\pi r^2 \rho} \quad (22)$$

$$\frac{dT}{dm} = -\frac{3}{4ac} \frac{\kappa}{T^3} \frac{L}{(4\pi r^2)^2} \quad (23)$$

$$\frac{dL}{dm} = q_0 \rho T^\nu \quad (24)$$

$$P = \frac{\mathcal{R}}{\mu} \rho T \quad (25)$$

The unknowns are  $r(m)$ ,  $P(m)$ ,  $T(m)$ ,  $L(m)$ , and  $\rho(m)$ , and there are 5 equations, so the system is fully specified.

We don't have to solve the equations exactly to get out the basic behaviour. Instead, we can figure out many scalings with some simple dimensional arguments. To do this, we will deploy the same technique of non-dimensionalising the equations that we used so effectively with polytropes. We begin by defining a dimensionless mass variable

$$x = \frac{m}{M}, \quad (26)$$

and then defining dimensionless versions of all the other variables:

$$r = f_1(x) R_* \quad (27)$$

$$P = f_2(x) P_* \quad (28)$$

$$\rho = f_3(x) \rho_* \quad (29)$$

$$T = f_4(x) T_* \quad (30)$$

$$L = f_5(x) L_*, \quad (31)$$

where  $M$  is the total mass of the star and  $R_*$ ,  $P_*$ ,  $\rho_*$ ,  $T_*$ , and  $L_*$  are values of the radius, pressure, density, temperature and luminosity that we have not yet specified.

Thus far all we have done is define a new set of variables. We will now substitute this new set of variables into the equation of hydrostatic balance:

$$\frac{dP}{dm} = -\frac{Gm}{4\pi r^4} \quad \longrightarrow \quad \frac{P_*}{M} \frac{df_2}{dx} = -\frac{GMx}{4\pi R_*^4 f_1^4}. \quad (32)$$

We now exercise our freedom to define  $P_*$ . We define it by

$$P_* = \frac{GM^2}{R_*^4}, \quad (33)$$

and with this choice the equation of hydrostatic balance reduces to

$$\frac{df_2}{dx} = -\frac{x}{4\pi f_1^4}. \quad (34)$$

This is the non-dimensional version of the equation.

We can non-dimensionalise the other equations in a similar fashion, in each case exercising our freedom to choose one of the starred quantities. For the  $dr/dm$  equation, we choose

$$\rho_* = \frac{M}{R_*^3}, \quad (35)$$

which gives us the non-dimensional equation

$$\frac{df_1}{dx} = \frac{1}{4\pi f_1^2 f_3}. \quad (36)$$

For the other equations, the definitions and non-dimensionalised versions are

$$T_* = \frac{\mu P_*}{\mathcal{R} \rho_*} \quad f_2 = f_3 f_4 \quad (37)$$

$$L_* = \frac{ac}{\kappa} \frac{T_*^4 R_*^4}{M} \quad \frac{df_4}{dx} = -\frac{3f_5}{4f_4^3 (4\pi f_1^2)^2} \quad (38)$$

$$L_* = q_0 \rho_* T_*^\nu M \quad \frac{df_5}{dx} = f_3 f_4^\nu. \quad (39)$$

You might be suspicious that we defined  $L_*$  twice, which we can't do. The trick is that we have yet not chosen  $R_*$ . Thus we can use our last choice to define  $R_*$  in such a way as to make the second equation here true. Once we do so, we have defined all the starred quantities, and non-dimensionalised all the equations.

What is the point of this? The trick is that the non-dimensional equations for  $f_1 - f_5$  now depend only on dimensionless numbers, and not on the stellar mass. Any dependence of the solution on mass *must* enter only through the starred quantities. Another way of putting it is that these equations have the property that they are homologous – one can solve for  $f_1 - f_5$ , and then scale that solution to an arbitrary mass by picking a different value of  $M$ . In a sense, these equations say that all stars have the same structure.

Of course in reality that's not quite true. The only reason we were able to obtain non-dimensionalised equations of this form and demonstrate homology is due to the simplifying assumptions we made – neglect of radiation pressure, neglect of convection, adopting a constant  $\kappa$ , and using a powerlaw form for the nuclear energy generation rate. These complications are the basic reasons that stars do not actually all have the same structure independent of mass. Nonetheless, the first and last of these assumptions are reasonably good for low mass stars (though not for massive stars). The assumption of constant  $\kappa$  isn't strictly necessary, as a powerlaw approximation for it still allow non-dimensionalisation in this way. The most questionable assumption is our neglect of convection.

## B. Mass scalings

With that aside out of the way, we can proceed to use the homologous equations to deduce the dependence of all quantities on mass. Combining the equations for  $\rho_*$  and  $T_*$  gives

$$T_* = \frac{\mu}{\mathcal{R}} \frac{GM}{R_*}. \quad (40)$$

Notice that we have already proven essentially this result using the virial theorem.

Inserting  $T_*$  into the equation for  $L_*$  gives

$$L_* = \frac{ac}{\kappa} \frac{R_*^4}{M} \left( \frac{\mu}{\mathcal{R}} \frac{GM}{R_*} \right)^4 = \frac{ac}{\kappa} \left( \frac{\mu G}{\mathcal{R}} \right)^4 M^3 \quad (41)$$

Since this relation applies at any value of  $x$ , it must apply at  $x = 1$ , i.e. at the surface of the star. Since at the stellar surface  $L = L_* f_5(1)$ , it immediately follows that

$$L \propto \frac{ac}{\kappa} \left( \frac{\mu G}{\mathcal{R}} \right)^4 M^3. \quad (42)$$

Thus the luminosity varies as  $M^3$ . Notice that this is independent of any of the other starred quantities – we have derived the dependence of  $L$  on the mass alone. Also notice that this result is basically the same as we get from Eddington’s model with  $\beta = 1$  (i.e., our assumption of no radiation pressure) – which makes sense, since Eddington’s model is a polytrope, and therefore homologous, and also has constant  $\kappa$ . Thus we couldn’t possibly find anything else.

We can now push further and deduce the mass scalings of other quantities as well. We have

$$L_* = q_0 \rho_* T_*^\nu M = \frac{ac}{\kappa} \left( \frac{\mu G}{\mathcal{R}} \right)^4 M^3 \quad \implies \quad \rho_* = \frac{ac}{q_0 \kappa} \left( \frac{\mu G}{\mathcal{R}} \right)^4 \frac{M^2}{T_*^\nu}. \quad (43)$$

Substituting for  $\rho_*$  and  $T_*$  gives

$$\frac{M}{R_*^3} = \frac{ac}{q_0 \kappa} \left( \frac{\mu G}{\mathcal{R}} \right)^4 M^2 \left( \frac{\mu P_*}{\mathcal{R} \rho_*} \right)^{-\nu} \quad (44)$$

Finally, substituting for  $P_*$  and  $\rho_*$  again gives

$$\frac{M}{R_*^3} = \frac{ac}{q_0 \kappa} \left( \frac{\mu G}{\mathcal{R}} \right)^4 M^2 \left( \frac{\mu}{\mathcal{R}} \right)^{-\nu} \left( \frac{GM^2 R_*^3}{R_*^4 M} \right)^{-\nu} \quad (45)$$

$$\frac{M}{R_*^3} = \frac{ac}{q_0 \kappa} \left( \frac{\mu G}{\mathcal{R}} \right)^{4-\nu} M^{2-\nu} R_*^\nu \quad (46)$$

$$R_* = \left[ \frac{q_0 \kappa}{ac} \left( \frac{\mathcal{R}}{\mu G} \right)^{4-\nu} \right]^{1/(\nu+3)} M^{(\nu-1)/(\nu+3)} \quad (47)$$

Thus we expect the stellar radius to scale with mass in a way that depends on how the nuclear reactions scale with temperature. If we have a star that burns hydrogen mainly via the  $pp$  chain, then  $\nu \approx 4$ , and we obtain  $R \propto M^{3/7}$ . For a more massive star that burns mainly via the CNO cycle, we have  $\nu \approx 20$ , and we instead obtain  $R \propto M^{19/23}$ , a nearly linear relationship. Thus we expect the radius to increase with mass as  $M^{3/7}$  at small masses, increasing in steepness to a nearly linear relationship at larger masses.

For the density, we have

$$\rho_* = \frac{M}{R_*^3} = \left[ \frac{q_0 \kappa}{ac} \left( \frac{\mathcal{R}}{\mu G} \right)^{4-\nu} \right]^{-3/(\nu+3)} M^{2(3-\nu)/(3+\nu)}. \quad (48)$$



For  $pp$  chain stars, this gives  $\rho_* \propto M^{-2/7}$ , and for CNO cycle stars it gives  $\rho_* \propto M^{-34/23}$ , which is nearly  $-1.5$ . Thus the density always decreases with increasing stellar mass, but does so fairly slowly for  $pp$  chain stars ( $-0.29$  power) and quite rapidly for CNO cycle stars ( $-1.5$  power). This is an important and often underappreciated point in stellar structure: more massive stars are actually much less dense than less massive ones. Very massive stars are quite puffy and diffuse.

### C. The observed main sequence

Finally, we can get out the scaling that we really care about: luminosity versus temperature. This is what will determine the shape of the observed main sequence, and we had better make sure that what we get out of the theoretical model agrees reasonably well with what we actually observe. If not, the hypothesis that the main sequence is made up of stars whose cores are stalled on the hydrogen burning line will not be valid.

The effective temperature is related to the radius and luminosity by

$$\frac{L}{4\pi R^2 \sigma} = T_{\text{eff}}^4. \quad (49)$$

However we have just shown that

$$L \propto M^3 \quad \text{and} \quad R \propto M^{(\nu-1)/(\nu+3)}. \quad (50)$$

Inverting the first relation and substituting it into the second, we have

$$M \propto L^{1/3} \quad \implies \quad R \propto (L^{1/3})^{(\nu-1)/(\nu+3)} \propto L^{(\nu-1)/[3(\nu+3)]}. \quad (51)$$

Now plugging this into the relationship between  $L$  and  $T_{\text{eff}}$ , we give

$$\frac{L}{[L^{(\nu-1)/[3(\nu+3)]}]^2} \propto T_{\text{eff}}^4 \quad (52)$$

$$L^{1-2(\nu-1)/[3(\nu+3)]} \propto T_{\text{eff}}^4 \quad (53)$$

$$\left[1 - \frac{2(\nu-1)}{3(\nu+3)}\right] \log L = 4 \log T_{\text{eff}} + \text{constant} \quad (54)$$

$$\log L = 4 \left[1 - \frac{2(\nu-1)}{3(\nu+3)}\right]^{-1} \log T_{\text{eff}} + \text{constant}. \quad (55)$$

We have therefore derived an equation for the slope that the main sequence should have in the HR diagram, which shows  $\log L$  vs.  $\log T_{\text{eff}}$ .

Plugging in  $\nu = 4$  for  $pp$  chain stars and  $\nu = 20$  for CNO cycle stars, we obtain

$$\log L = 5.6 \log T_{\text{eff}} + \text{constant} \quad (pp \text{ chain}) \quad (56)$$

$$\log L = 8.9 \log T_{\text{eff}} + \text{constant} \quad (\text{CNO cycle}) \quad (57)$$

The values compare reasonably well with the observed slopes of the lower and upper main sequence on the HR diagram.

## III. Numerical results

We have now pushed as far as we are going to analytically, and the time has come to bring out the computers. We have written down all the necessary equations, and they can be

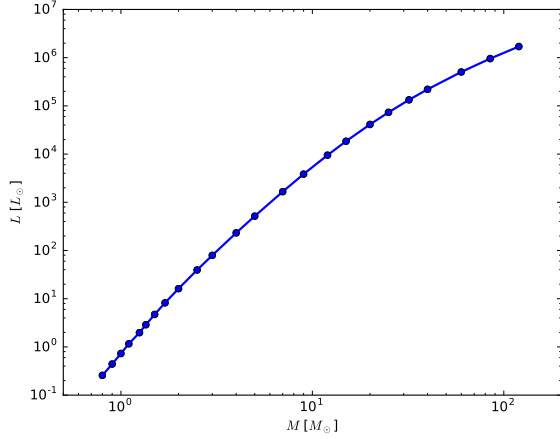


Figure 4: Luminosity versus mass for zero age stars of Solar composition, as predicted by the Geneva group. The tracks used to generate these plots were taken from the work of Ekstrom et al. (2012, <http://adsabs.harvard.edu/abs/2012A%26A...537A.146E>).

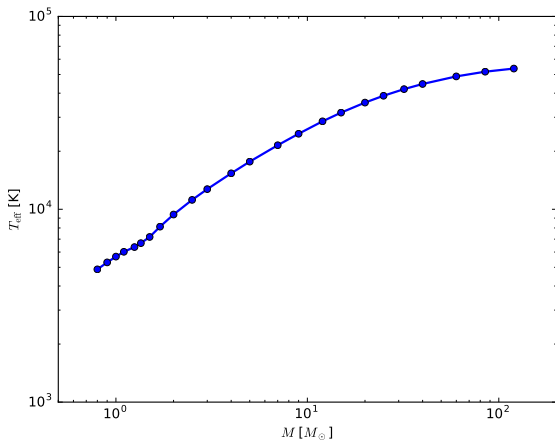


Figure 5: Same as Figure 4, but not showing  $T_{\text{eff}}$  versus mass.

solved by modern computers quite easily. We will not discuss the necessary algorithms – a 6 week course is too short for that. Instead, we will simply review the important results. For today we will focus on stars that have not yet processed a significant amount of hydrogen into helium. Stars of this sort are said to be on the zero age main sequence, or ZAMS for short. We will talk about evolution of stars after the ZAMS in the remaining classes.

#### A. Mass-luminosity-effective temperature relations

The most basic output of the numerical codes is a prediction for the luminosity and effective temperature of a star of a given mass and composition. Numerical tabulations of predictions for this quantity are available from a number of research groups, all using slightly different treatments of convection and similar effects that cannot quite be modelled exactly in a 1D code. The figures shown here are models from the Geneva Observatory group. Figure 4 shows the mass-luminosity relation, Figure 5 shows mass versus effective temperature, and Figure 6 shows luminosity versus effective temperature.

The basic behaviour is essentially as we predicted from our simple models. The luminosity scales as mass to roughly the third power at low masses – slightly steeper due both to the effects of convection and the varying opacity. At higher masses the dependence flattens out, approaching  $L \propto M$  at the very highest masses. The most massive stars have luminosities of a bit more than  $10^6 L_{\odot}$ . Similarly, the plot of  $\log L$  vs.  $\log T_{\text{eff}}$  has a slope of  $\sim 5 - 6$  for intermediate mass stars, with values

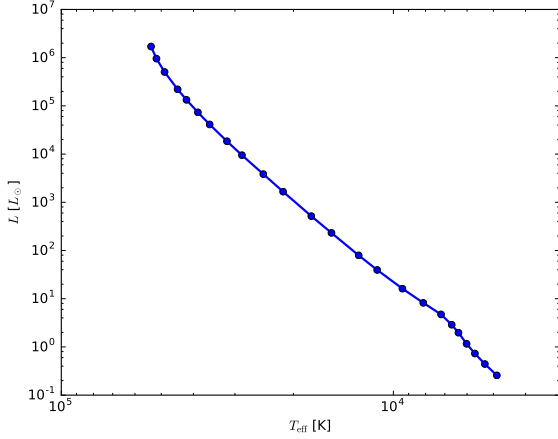


Figure 6: Same as Figure 4, but not showing  $L$  versus  $T_{\text{eff}}$ .

of the effective temperature ranging from a few thousand Kelvin to several tens of thousands.

## B. Interior structure and convection

Another basic output of the numerical models is a prediction the internal structure of stars, meaning the run of density, mass, temperature, pressure, etc. versus radius, plots of where stars are convective and where they are not, and where in their interiors they produce nuclear energy, and via which channels.

One interesting a non-obvious point that emerges from the numerical models involves convection: the behaviour of where stars are convective is somewhat complicated. Very low mass stars, those below  $\sim 0.3 M_{\odot}$ , are convective essentially everywhere in their interiors. The basic reason for this is that their low temperatures make their opacities quite high, so convection is required to carry the stellar luminosity.

As one increases the mass, the convective region moves away from the centre of the star, which becomes hot enough for the opacity to go down and radiation to carry the flux. For a star like the Sun, convection only occurs in the outer layers of the star, which are cooler. Consequently, only the outer  $\sim 10\%$  of the mass is convective, though this mass, because it is at low density, occupies a significant fraction of the star's radius.

As one increases mass still further, the convection zone in the outer parts of the star gets smaller and smaller due to increasing temperature, but the centre of the star becomes convective. This convection is a result of the CNO cycle turning on. The CNO cycle is very sensitive to temperature (recall that  $q_{\text{nuc}} \sim T^{20}$ ), and this produces a very steep gradient in temperature. Steep temperature gradients favour convection. Thus stars with masses of  $\approx 10 M_{\odot}$  wind up having convection in the inner  $\approx 50\%$  of their mass, with no convection in their outer layers.